1-21-2014

Analysis of Localized Diabatic States beyond the Condon Approximation for Excitation Energy Transfer Processes

Ethan Alguire

Shervin Fatehi
University of Texas Rio Grande Valley, shervin.fatehi@utrgv.edu

Yihan Shao

Joseph E. Subotnik
University of Pennsylvania

Recommended Citation

Alguire, E. C.; Fatehi, S.; Shao, Y.; Subotnik, J. E. Analysis of Localized Diabatic States Beyond the Condon Approximation for Excitation Energy Transfer Processes. J. Phys. Chem. A 2014, 118, 11891– 11900, DOI: 10.1021/jp411107k

An analysis of localized diabatic states beyond the Condon approximation for excitation energy transfer processes

Ethan C. Alguire,* Shervin Fatehi, Yihan Shao,† and Joseph E. Subotnik‡

Dept. of Chemistry, 231 S. 34th Street,

University of Pennsylvania, Philadelphia, PA, 19104-6323

Dept. of Chemistry, 315 S. 1400 E. Rm. 2020,

University of Utah, Salt Lake City, UT 84112-0850 and

Q-Chem, Inc., 6601 Owens Drive, Suite 105, Pleasanton, CA 94588

In a previous paper [Fatehi, S. *et al. J. Chem. Phys.* **2013**, *139*, 124112], we demonstrated a practical method by which analytic derivative couplings of Boys-localized CIS states can be obtained. In this paper, we now apply that same method to the analysis of triplet-triplet energy transfer systems studied by Closs and collaborators [Closs, G. L. *et al. J. Am. Chem. Soc.* **1988**, *110*, 2652]. For the systems examined, we are able to conclude that (i) the derivative coupling in the BoysOV basis is negligible, and (ii) the diabatic couplings will likely change little over the configuration space explored at room temperature. Furthermore, we propose and evaluate an approximation which allows for the inexpensive calculation of accurate diabatic energy gradients, called the 'strictly diabatic' approximation. This work highlights the effectiveness of diabatic state analytic gradient theory in realistic systems, and demonstrates that localized diabatic states can serve as an acceptable approximation to strictly diabatic states.

I. INTRODUCTION

The ability to properly model nonadiabatic dynamics is essential for understanding innumerable chemical systems.[1] Problems in the field of nonadiabatic dynamics are commonly approached, at least in a conceptual framework, from the perspective of the strictly diabatic electronic representation. Strictly diabatic wavefunctions ($\{|\Xi_A\rangle\}$) are defined by the characteristic that they are not coupled to each other by nuclear momentum, or in other words, that the derivative couplings (DCs) are zero,

$$d_{AB}^{[Q]} = \langle \Xi_A | \nabla_Q | \Xi_B \rangle = 0, \tag{1}$$

where Q indexes a nuclear degree of freedom. While they are not coupled by nuclear momentum, diabatic states are coupled by elements of the electronic Hamiltonian (H_{AB}) called diabatic couplings. If this Hamiltonian is diagonalized, of course, one obtains the adiabatic basis of electronic states. The cost of this transformation is that the derivative couplings in the new basis are inversely proportional to the energy difference between the states that they couple ($d_{IJ}^{[Q]} \propto (E_J - E_I)^{-1}$), and can therefore become large near avoided crossings and diverge near conical intersections.

While a strictly diabatic basis would be useful, in practice it is impossible to obtain.[2,3] In its place, numerous approximations (called simply 'diabatic' states) have been proposed. One approach is to directly minimize DCs along a given reaction path.[4] In more recent years, Yarkony has proposed a method that can minimize derivative couplings for small- to medium-sized systems.[5,6] Other methods approximate diabatic states by constructing a

*Electronic address: alguire@sas.upenn.edu

†Electronic address: yihan.shao@gmail.com

‡Electronic address: subotnik@sas.upenn.edu

basis in which the states change little with respect to nuclear motion; such methods include Pacher, Cederbaum, and Köppel's block diagonalization[7], Atchity, Ruedenberg, *et al.*'s configurational uniformity[8,9], and Nakamura and Truhlar's fourfold way.[10–12] Other techniques approach the problem more obliquely; the Generalized Mulliken-Hush (GMH) algorithm of Cave and Newton[13,14] approximates diabatic states as eigenstates of a component of the dipole operator, utilizing the heuristic property that diabatic states for electron transfer (ET) processes tend to be localized in space. The idea that singular derivative couplings could be removed by obtaining the eigenstates of an observable was later formally demonstrated by Yarkony.[15–17] Other examples of techniques which produces diabatic states by localizing wavefunctions include Voityuk's fragment charge difference (FCD) method[18] and Hsu's extension of FCD to excitation energy transfer (EET) systems, called fragment excitation difference (FED).[19–21] The concept of charge localization in ET states was also applied to the construction of diabatic densities in the context of density functional theory (DFT) by Van Voorhis *et al.*[22–24] For comprehensive reviews on this topic, see Refs. 3 and 25. The current work is concerned with localized diabatization schemes[26–29], for which diabatic ET and EET states can be approximated by a linear combination of adiabatic states determined by minimizing a functional of the electronic subspace. Hereafter, any reference to diabatic states will refer to localized diabatic states.

As discussed in previous publications[29,30], localized diabatic states could potentially be used with several nonadiabatic dynamics methods[31,32], especially those that are agnostic to electronic representation.[33–36] In order to propagate dynamics in a localized diabatic representation, it is necessary to have an efficient way to determine diabatic gradient quantities; it would be even better to establish that derivative couplings in such a representation are negligible for a particular system. Additionally, localized diabatization methods have been

used in the context of Marcus theory to accurately model[28] the rate of triplet-triplet EET in systems studied by Closs *et al.*[37,38] While theoretical and experimental results agreed reasonably well, until now we have not been able to prove beyond doubt that this success was not coincidental. After all, Marcus theory is formally applicable only to strictly diabatic states.

In this manuscript, we use our newly-developed analytic gradient theory for diabatic states[30] to reexamine the validity of locally diabatic states and to ascertain definitively whether the Closs systems conform to the approximations of Marcus theory. With these considerations in mind, first, we compare the DCs of these molecules in the adiabatic and diabatic representations. If the diabatic states are similar to the strictly diabatic states postulated by Marcus, one should expect that their DCs are insignificant even near avoided crossings. Second, we use diabatic Hamiltonian gradients to estimate how much the diabatic coupling changes within the configuration space available to these systems at room temperature. Marcus theory assumes the Condon approximation, which posits that the diabatic couplings do not change significantly, and we show that it holds true here. Third and finally, in the discussion section, we will present and evaluate an approximation which can produce diabatic state gradient quantities at the cost of producing adiabatic derivative couplings.

II. NOTATION

The uppercase letters $\{I, J, K, L\}$ index adiabatic electronic states, while $\{A, B, C, D\}$ are used to index diabatic electronic states. The lowercase letters $\{i, j\}$ index occupied molecular orbitals, while $\{a, b\}$ index virtual molecular orbitals. Following the convention established in Ref. 39, nuclear degrees of freedom in the Cartesian basis are indexed by the letter Q, and gradients with respect to such degrees of freedom are denoted by a superscript Q enclosed

in square brackets, such as $f^{[Q]}$. Nuclear degrees of freedom in the basis of normal modes are indexed by the letter η, and gradients are similarly represented as superscripts enclosed in brackets, e.g. $f^{[\eta]}$. Quantities that feature R in the same context ($\mathbf{f}^{[R]}$) denote gradients over all nuclear degrees of freedom. Diabatic states are denoted $|\Xi\rangle$, adiabatic states are denoted $|\Phi\rangle$, and derivative couplings are denoted $d_{IJ}^{[Q]}$. All other terms are explained as they arise.

III. THEORY

A. Localized diabatization

The localized diabatization method is an inexpensive, black-box method for generating a diabatic electronic basis as a linear combination of adiabatic states. Localized diabatic states are obtained by mixing a basis of M adiabatic states via an adiabatic-to-diabatic transformation matrix $\mathbf{U}$, such that

$$|\Xi_A\rangle = \sum_{I=1}^{M} U_{AI}|\Phi_I\rangle, \tag{2}$$

where $\mathbf{U}$ is chosen (1) to be unitary, ensuring orthonormal diabats, and (2) to maximize some diabatization function. Two such functions, Boys and BoysOV localization, depend on state dipole operators. These two methods are direct descendants of GMH[13], which uses the dipole operator as a guide to producing fully localized states. Specifically, diabatic states in the GMH representation must have a dipole operator that is diagonalized in the direction of charge transfer. Boys diabatization represents an extension of this method to multiple centers of charge, and in fact reduces to GMH for two-state systems.[26] In principle, Boys diabatic states can be thought of as adiabatic states perturbed by the approximate effects of a strongly localizing solvent bath, one which exerts a linear electrostatic potential on the

electronic system being diabatized. Consequently, maximizing this interaction is equivalent to maximizing the localization function f_{Boys}, given by

$$f_{\text{Boys}}(\mathbf{U}) = f_{\text{Boys}}(\{\Xi_A\}) \tag{3}$$

$$= \sum_{A,B=1}^{M} |\langle \Xi_A|\boldsymbol{\mu}|\Xi_A\rangle - \langle \Xi_B|\boldsymbol{\mu}|\Xi_B\rangle|^2, \tag{4}$$

where $\boldsymbol{\mu}$ is the electronic dipole operator. Boys diabatic states are useful for localizing ET states, but are subject to certain limitations. In particular, the Boys method is unable to localize the electronic states of an EET system, in which electronic excitation, not charge, becomes localized. An alternative method, called BoysOV localization[28], uses a diabatization function given by

$$f_{\text{BoysOV}}(\mathbf{U}) = \sum_{A,B=1}^{M} |\langle \Xi_A|\boldsymbol{\mu}^{\text{occ}}|\Xi_A\rangle - \langle \Xi_B|\boldsymbol{\mu}^{\text{occ}}|\Xi_B\rangle|^2 \tag{5}$$

$$+ |\langle \Xi_A|\boldsymbol{\mu}^{\text{virt}}|\Xi_A\rangle - \langle \Xi_B|\boldsymbol{\mu}^{\text{virt}}|\Xi_B\rangle|^2, \tag{6}$$

where the dipole operators $\boldsymbol{\mu}^{\text{occ}}$ and $\boldsymbol{\mu}^{\text{virt}}$ only interact with occupied and virtual orbital densities, respectively. For CIS states, this means

$$\langle \Xi_A|\boldsymbol{\mu}^{\text{occ}}|\Xi_B\rangle = \boldsymbol{\mu}^{\text{occ}}_{AB} = -\sum_{i,j,a} t_i^{A,a} t_j^{B,a} \boldsymbol{\mu}_{ij} \tag{7}$$

and

$$\langle \Xi_A|\boldsymbol{\mu}^{\text{virt}}|\Xi_B\rangle = \boldsymbol{\mu}^{\text{virt}}_{AB} = \sum_{i,a,b} t_i^{A,a} t_i^{B,b} \boldsymbol{\mu}_{ab}, \tag{8}$$

where we have introduced CIS amplitudes $\{t\}$. By separately localizing these two types of electron densities, BoysOV allows for the localization of excitations for a given set of states, even if charge cannot be localized for the same subspace. Formally, BoysOV can be easily applied to CIS or time-dependent density functional theory under the Tamm-Dancoff approximation (TD-DFT/TDA), but further generalizations are possible (see Appendix A).

B. Derivative couplings between localized diabatic states

The formal expression for derivative couplings between localized diabatic states can be written simply as

$$d_{AB}^{[Q]} = \sum_{I} U_{AI} d_{IJ}^{[Q]} U_{BJ} + U_{AI} U_{BI}^{[Q]}. \tag{9}$$

Expressions for the derivative couplings[40–46] and gradients[47–51] of CI adiabatic states are available, and we have described methods for obtaining analytic derivative couplings between adiabatic states within the CIS formalism.[39] To calculate any gradient quantity within a diabatic representation also requires the transformation matrix gradient, $\mathbf{U}^{[R]}$. The process for calculating $\mathbf{U}^{[R]}$ for Boys diabatic states is described in detail in Ref. 30. Here, we will broadly describe the process for the three localized diabatization schemes that make use of dipole operators: GMH, Boys, and BoysOV localization. In each case, there are two groups of constraints on the diabatic states which can be used to construct a supermatrix equation,

$$\sum_{CK} \begin{bmatrix} \mathcal{A}_{ABCK} \\ \mathcal{B}_{ABCK} \end{bmatrix} U_{CK}^{[Q]} = - \begin{bmatrix} \mathbf{0} \\ \mathcal{C}_{AB}^{[Q]} \end{bmatrix}, \tag{10}$$

which can subsequently be solved to obtain $\mathbf{U}^{[R]}$. The first set of constraints,

$$\sum_{CK} \mathcal{A}_{ABCK} U_{CK}^{[Q]} = \mathbf{0}, \tag{11}$$

arises from the condition that diabatic states must be orthonormal,

$$\sum_{I} U_{AI} U_{BI} = \delta_{AB}. \tag{12}$$

If we take the gradient of Eq. 12 with respect to nuclear degrees of freedom Q, we obtain

$$\sum_{I} U_{AI}^{[Q]} U_{BI} + \sum_{I} U_{AI} U_{BI}^{[Q]} = 0, \tag{13}$$

which holds for all state pairs $A \geq B$. This result can be rearranged in the form of Eq. 11, where $\mathcal{A}_{ABCK} = \delta_{AC} U_{BK} + \delta_{BC} U_{AK}$.

While the unitarity condition is true for all localized diabatization schemes, in order to fully define the M^2 elements of $\mathbf{U}^{[Q]}$ we must turn to the second set of constraints,

$$\sum_{CK} \mathcal{B}_{ABCK} U^{[Q]}_{CK} = -\mathcal{C}^{[Q]}_{AB}, \tag{14}$$

which involve conditions specific to each scheme. By definition[13], GMH states must be constructed such that for $M = 2$,

$$\boldsymbol{\mu}_{AB} \cdot (\boldsymbol{\mu}_{11} - \boldsymbol{\mu}_{22}) = 0 \tag{15}$$

where $\boldsymbol{\mu}_{11}$ and $\boldsymbol{\mu}_{22}$ are diagonal elements of the dipole operator in the adiabatic basis, localized on the two different charge centers associated with the ET reaction. Taking the gradient of Eq. 15 with respect to nuclear degrees of freedom Q again allows us to express $\mathbf{U}^{[R]}$ in the context of a supermatrix equation (Eq. 14), for which

$$\mathcal{B}^{\mathrm{GMH}}_{ABCK} = \sum_{CK} \delta_{AC} \boldsymbol{\mu}_{BK} \cdot (\boldsymbol{\mu}_{11} - \boldsymbol{\mu}_{22}) \tag{16}$$

$$+\delta_{BC} \boldsymbol{\mu}_{AK} \cdot (\boldsymbol{\mu}_{11} - \boldsymbol{\mu}_{22}) \tag{17}$$

and

$$\mathcal{C}^{\mathrm{GMH}[Q]}_{AB} = \sum_{IJ} \left[\boldsymbol{\mu}^{[Q]}_{IJ} \cdot (\boldsymbol{\mu}_{11} - \boldsymbol{\mu}_{22}) + \boldsymbol{\mu}_{IJ} \cdot \left(\boldsymbol{\mu}^{[Q]}_{11} - \boldsymbol{\mu}^{[Q]}_{22} \right) \right] U_{AI} U_{BJ}. \tag{18}$$

A similar approach is used to define the constraints on $\mathbf{U}^{[R]}$ for the Boys representation. It can be shown[26] that the condition

$$\boldsymbol{\mu}_{AB} \cdot (\boldsymbol{\mu}_{AA} - \boldsymbol{\mu}_{BB}) = 0 \tag{19}$$

must be obeyed for all state pairs such that $A > B$. The gradient of this expression can then be taken and the result can be written in the form of Eq. 14 with

$$\mathcal{B}^{\mathrm{Boys}}_{ABCK} = \sum_{CK} \delta_{AC} \left[2\boldsymbol{\mu}_{AB} \cdot \boldsymbol{\mu}_{KA} + (\boldsymbol{\mu}_{AA} - \boldsymbol{\mu}_{BB}) \cdot \boldsymbol{\mu}_{KB} \right] \tag{20}$$

$$-\delta_{BC} \left[2\boldsymbol{\mu}_{AB} \cdot \boldsymbol{\mu}_{KB} - (\boldsymbol{\mu}_{AA} - \boldsymbol{\mu}_{BB}) \cdot \boldsymbol{\mu}_{KA} \right] \tag{21}$$

and

$$\mathcal{C}_{AB}^{\mathrm{Boys}[Q]} = \sum_{IJKL} \left[\boldsymbol{\mu}_{IJ}^{[Q]} \cdot \boldsymbol{\mu}_{KL} + \boldsymbol{\mu}_{IJ} \cdot \boldsymbol{\mu}_{KL}^{[Q]} \right] U_{AI} U_{BJ} \left(U_{BK} U_{BL} - U_{AK} U_{AL} \right). \tag{22}$$

We can easily extend the form of this supermatrix expression to BoysOV localization if we instead require that the condition

$$\boldsymbol{\mu}_{AB}^{\mathrm{occ}} \cdot \left(\boldsymbol{\mu}_{AA}^{\mathrm{occ}} - \boldsymbol{\mu}_{BB}^{\mathrm{occ}} \right) + \boldsymbol{\mu}_{AB}^{\mathrm{virt}} \cdot \left(\boldsymbol{\mu}_{AA}^{\mathrm{virt}} - \boldsymbol{\mu}_{BB}^{\mathrm{virt}} \right) = 0 \tag{23}$$

must be satisfied. This 'BoysOV condition' is simply the Boys condition divided into separate parts for the occupied and virtual contributions to the dipole operator. The resulting supermatrices, represented as functions of the dipole operators, can be written

$$\mathcal{B}^{\mathrm{BoysOV}} = \mathcal{B}^{\mathrm{Boys}} \left(\boldsymbol{\mu}^{\mathrm{occ}} \right) + \mathcal{B}^{\mathrm{Boys}} \left(\boldsymbol{\mu}^{\mathrm{virt}} \right), \tag{24}$$

and

$$\mathcal{C}^{\mathrm{BoysOV}[Q]} = \mathcal{C}^{\mathrm{Boys}[Q]} \left(\boldsymbol{\mu}^{\mathrm{occ}} \right) + \mathcal{C}^{\mathrm{Boys}[Q]} \left(\boldsymbol{\mu}^{\mathrm{virt}} \right). \tag{25}$$

The supermatrices necessary for obtaining $\mathbf{U}^{[R]}$ exist in a small-dimensional state space, so inverting Eq. 10 is computationally trivial. The costly part of obtaining diabatic gradient quantities is filling in the constraint matrix $\mathcal{C}^{[R]}$ with adiabatic dipole gradients $\boldsymbol{\mu}^{[R]}$. Note that although the cost of calculating $\mathcal{C}^{[R]}$ for GMH is equivalent to the same procedure for Boys diabatic states, the cost for BoysOV is twice as great, as each quantity must be calculated once for virtual densities and once for occupied densities. Consequently, for a two-state calculation, the cost of this procedure for BoysOV states should be approximately twenty times the cost of a CIS gradient.[30]

C. Diabatic Hamiltonian gradient and the strictly diabatic approximation

In addition to producing diabatic-basis derivative couplings, the transformation matrix gradient $\mathbf{U}^{[R]}$ can be used to produce any diabatic gradient quantity. Among these quantities,

the diabatic Hamiltonian gradient $\mathbf{H}^{[R]}$ is of primary interest. As with the expression for the derivative coupling (Eq. 9), the expression for the Hamiltonian gradient is simple,

$$H_{AB}^{[Q]} = \sum_{IJ} U_{AI} H_{IJ}^{[Q]} U_{BJ} + U_{AI}^{[Q]} H_{IJ} U_{BJ} + U_{AI} H_{IJ} U_{BJ}^{[Q]}. \tag{26}$$

From Eq. 26, one can calculate both energy gradients (diagonal elements) and diabatic coupling derivatives (off-diagonal elements). The gradients of any other observable can be represented by the same expression, by simply replacing the Hamiltonian with the Hermitian operator of interest.

As for derivative couplings, the most costly step in evaluating Eq. 26 is the calculation of $\mathbf{U}^{[R]}$. Reducing the cost of building the transformation matrix gradient would make building the energy gradients much less expensive, and therefore practical for larger molecules. One shortcut, which we dub the 'strictly diabatic' approximation, takes advantage of one of the principle desired properties of diabatic states: to have negligible derivative couplings. Formally assuming the strictly diabatic condition (Eq. 1) allows us to solve Eq. 9 for $\mathbf{U}^{[R]}$,

$$U_{AI}^{[Q]} = \sum_{J} U_{AJ} d_{JI}^{[Q]}. \tag{27}$$

If it can be demonstrated that localized diabatic states have small enough derivative couplings to make this a viable approximation, diabatic gradient quantities could be obtained for the cost of adiabatic derivative couplings, which would reduce calculation time by an order of magnitude.

IV. RESULTS

All results were calculated using a development version of the Q-CHEM software package.[52,53] Excited states were generated using the restricted Hartree-Fock configuration

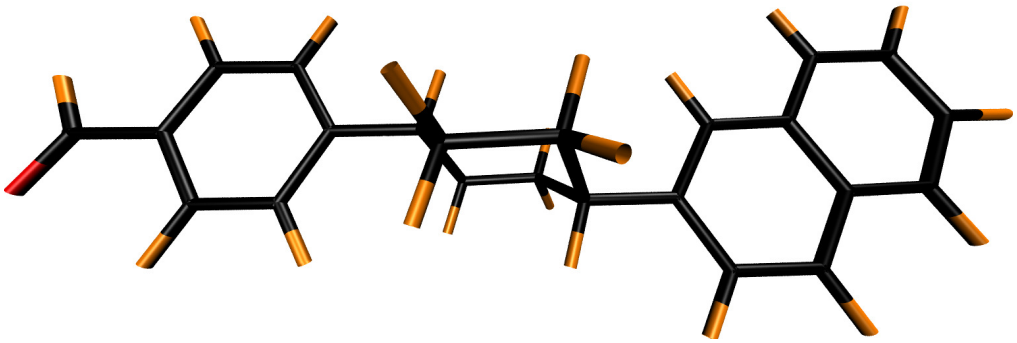

FIG. 1: The DBA molecule C-1,4ee has two minima on the T_1 surface associated with a triplet-triplet EET system. In the higher-energy local minimum configuration, the excitation is localized on the benzaldehydeyl donor (the AD* state). In the global minimum configuration for this surface, the excitation is localized on the 2-naphthyl acceptor (the A*D state). Here C-1,4ee is shown in the geometry optimized for the A*D configuration of the T_1 excited state.

interaction singles (RHF-CIS) formalism with a 6-31G** basis set. The systems under consideration are similar to those used in Ref. 37: each is a donor-bridge-acceptor (DBA) molecule in which a 4-benzaldehydeyl donor and a 2-naphthyl acceptor are joined to a variable bridge. Note that in the actual experiments, the donor is a benzophenoneyl group instead of a benzaldehydeyl group. We designate these molecules using the same naming scheme employed in Ref. 37; for example, C-1,3ea signifies a cyclohexane bridge to which the donor group is attached at carbon 1 equatorially, and to which the acceptor group is attached to carbon 3 axially. One such molecule, C-1,4ee, is pictured in Fig. 1. The space of configurations considered for each molecule is a reaction coordinate ζ defined as a linear interpolation between A*D ($\zeta = 0$) and AD* ($\zeta = 1$) energy-minimized geometries of the T_1 state. Normal modes are indexed by frequency, where mode 1 is the lowest-frequency mode.

A. Derivative coupling in the BoysOV representation

While the derivative coupling is of course a 3N-vector, for the purposes of analyzing the validity of Eq. 1 for BoysOV localized states, it is sufficient for our purposes to discuss

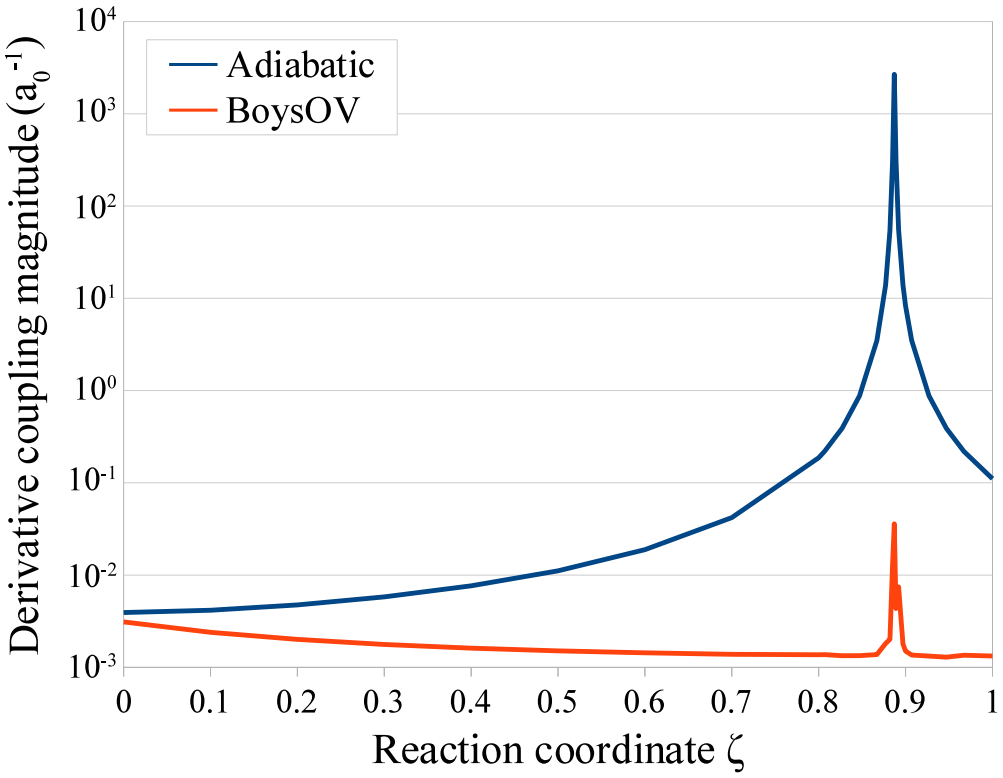

FIG. 2: Magnitudes of the DC vector along the linearly-interpolated reaction pathway between A*D ($\zeta = 0$) and AD* ($\zeta = 1$) T_1 states of the C-1,4ee molecule. DC magnitudes are presented in both the adiabatic and diabatic (BoysOV) bases. While the DC magnitude is smaller in the BoysOV basis for every point sampled, the degree of reduction is greatest near the avoided crossing, where it peaks at 2.7×10^3 a_0^{-1} in the adiabatic basis, and 3.6×10^{-2} a_0^{-1} in the diabatic basis. There is little difference between the adiabatic and diabatic representations far from the avoided crossing at $\zeta = 0$, where DC magnitudes are negligible in either representation.

the derivative coupling magnitudes alone. DC magnitudes in the adiabatic and BoysOV representations for C-1,4ee are shown in Fig. 2. This system is typical of the molecules considered in this study: the adiabatic DC magnitudes tend to be negligible near the endpoints of the reaction coordinate, but peak sharply near the avoided crossing. The DC magnitude is universally smaller in the BoysOV representation than it is in the adiabatic representation, particularly near the avoided crossing, where it is smaller by a factor of nearly 10^5. Just like the corresponding adiabatic quantity, the BoysOV DC magnitude peaks near the avoided crossing. However, it is not clear whether this peak is an accurate reflection of the BoysOV

TABLE I: Magnitudes of DCs between the triplet-triplet energy transfer states of three different Closs molecules in the adiabatic and diabatic (BoysOV) representations at the configuration nearest to the avoided crossing along the linearly-defined reaction coordinate ζ. These configurations represent the maximum DC magnitudes among the configurations sampled for each system, suggesting that the diabatic DCs are negligible over all relevant portions of configuration space for these systems.

	DC magnitude at avoided crossing point (a_0^{-1})		
Representation	C-1,3ea	C-1,3ee	C-1,4ee
Adiabatic	2500	970	2700
Diabatic	0.066	0.0078	0.036
A/D ratio	3.8×10^4	1.2×10^5	7.4×10^4

wavefunction behavior in this region: the coupled-perturbed Hartree-Fock (CPHF) response equations necessary for calculating BoysOV derivative couplings are particularly unstable here, requiring relaxed convergence criteria. As such, the four data points corresponding to the peak in the BoysOV DC magnitudes at the avoided crossing might be artificially large. Even with this practical limitation, the diabatic basis DC magnitude is still universally small, peaking at a value of 0.036 a_0^{-1}.

For a more general comparison, we have collected the magnitudes of the derivative couplings for several Closs systems near the avoided crossing point along the chosen reaction coordinate. This information is presented in Table I. As in the case of C-1,4ee, the avoided crossing point is where the DC magnitude peaks in each representation. In the diabatic representation, DC magnitude is reduced from the corresponding adiabatic value by at least four orders of magnitude in each case, and is never greater than 0.1 a_0^{-1}. As mentioned for the C-1,4ee system, it seems likely that the true DC magnitudes for BoysOV states are even smaller than the values presented here, although instabilities in the CPHF calculations and

finite precision error have likely inflated the size of the DC magnitudes near the avoided crossing.

B. Evaluating fluctuations in the diabatic coupling

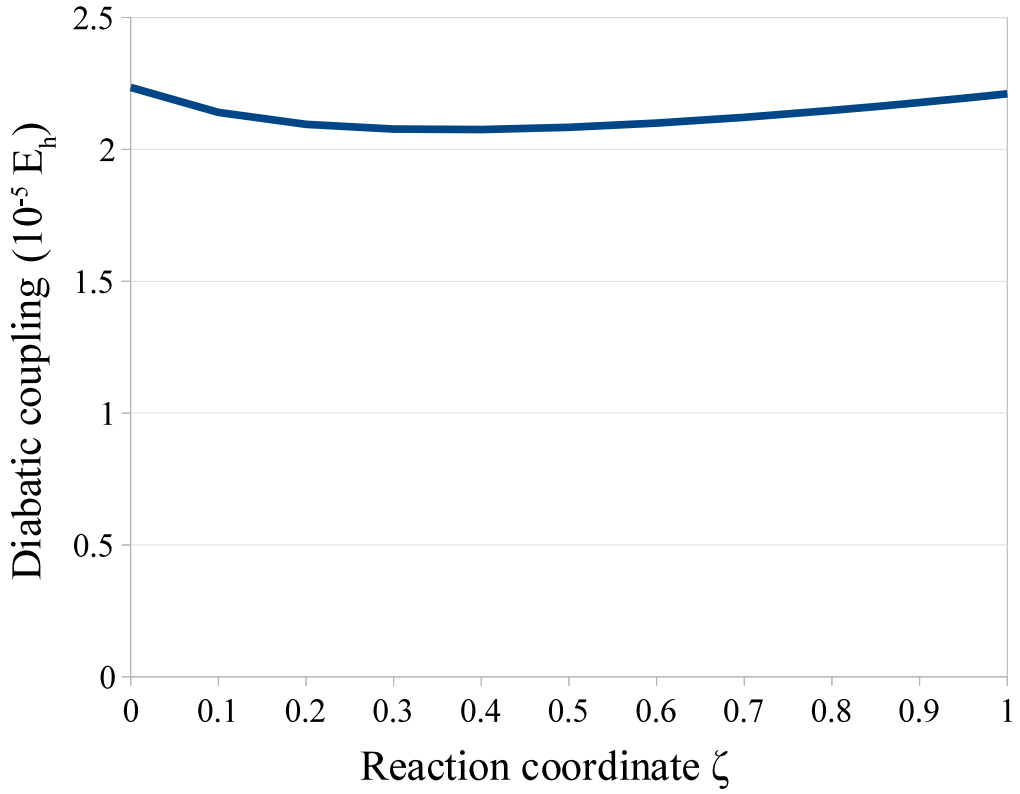

FIG. 3: Diabatic coupling along the linearly-interpolated reaction pathway between A*D ($\zeta = 0$) and AD* ($\zeta = 1$) T_1 states of the C-1,4ee molecule in the BoysOV representation. Among the points sampled, the maximum value (22.4 μE_h) and minimum value (20.8 μE_h) differ only by about 7% over the extent of the points sampled here, which constitute a change in nuclear degrees of freedom of about 0.88 a_0.

While the derivative coupling in the adiabatic representation appear to be tightly localized in space for these systems, the same is not necessarily true for diabatic coupling in the BoysOV representation. On the contrary, in the BoysOV representation, the diabatic coupling varies little along the reaction coordinate sampled in our study (Fig. 3); the difference between its maximum and minimum values is only 7%. At first glance, Fig. 3 would

seem to conform to the Condon approximation for this molecular system, and thus to the assumptions of Marcus theory (as explained in Refs. 54 and 55). Nevertheless, Fig. 3 is only a one-dimensional representation of the diabatic coupling. To understand multidimensional effects, in Fig. 4 we plot the norm of the diabatic coupling gradient ($|\mathbf{H}_{AB}^{[R]}|$, for $A \neq B$) as a function of the reaction coordinate. Although $|\mathbf{H}_{AB}^{[R]}|$ overlaps little with the reaction coordinate, should the molecule be displaced into some orthogonal mode, the diabatic coupling will not necessarily remain stable. Thus, it is worthwhile to explore whether this molecule is rigid enough at room temperature to avoid such conformational fluctuations as might change its diabatic coupling significantly.

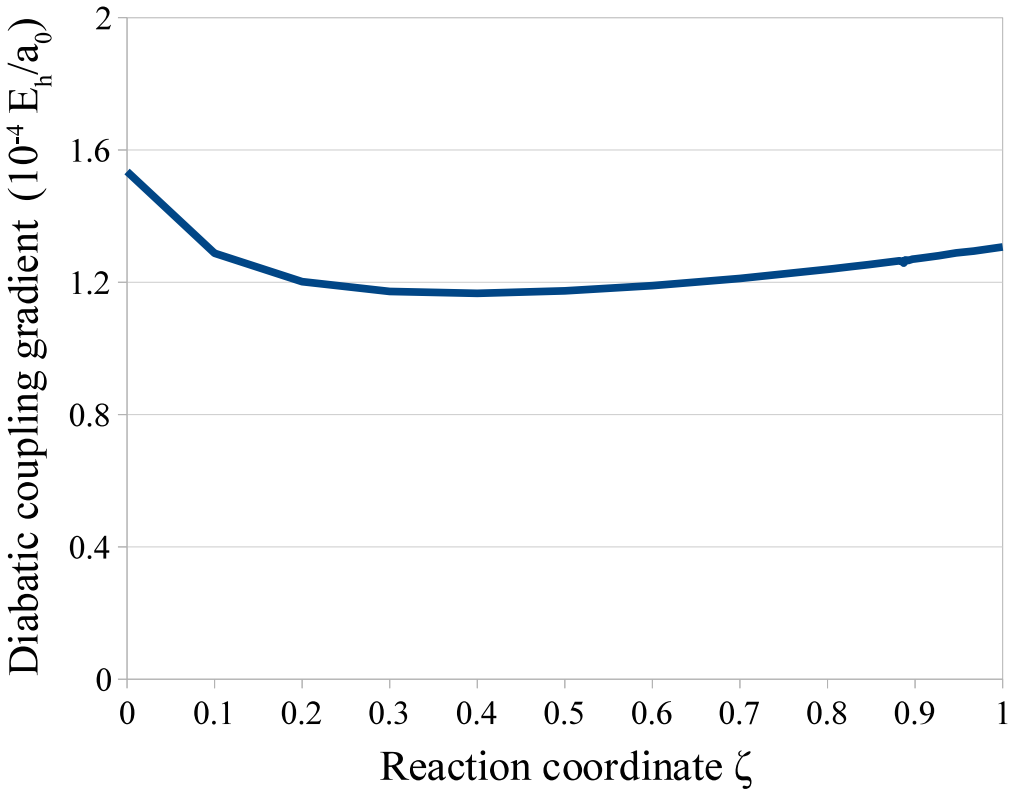

FIG. 4: Magnitude of the diabatic coupling gradient ($|\mathbf{H}_{AB}^{[R]}|$) along the linearly-interpolated reaction pathway between A*D ($\zeta = 0$) and AD* ($\zeta = 1$) T_1 states of the C-1,4ee molecule in the BoysOV representation. The magnitude of the gradient alone suggests that the diabatic couplings change by as much as 140 μE_h over the reaction pathway defined here (total length 0.88 a_0); however, as the graph of the diabatic coupling makes clear (Fig. 3), the diabatic coupling gradient overlaps little with the degree of freedom defined by the reaction coordinate.

To determine how much the diabatic coupling of this molecule might deviate due to conformational fluctuations, we must first estimate the probable conformational changes accessible to it at room temperature, and then combine this information with the diabatic coupling gradient. We can accomplish this goal in three steps: (1) for each minimum-energy geometry, we approximate the shape of the potential well as that of the minimum-energy ground state configuration. We can then use a Hessian calculation at the S_0 minimum-energy configuration to describe the normal modes and corresponding vibrational frequencies (ν_η) of the system. (2) Approximate the magnitude of configurational fluctuations (ΔL_η) with respect to this degree of freedom by taking the square root of the thermal average of the squared displacement operators along these modes,

$$\Delta L_\eta = \sqrt{\sum_m P_m \Delta X_{\eta,m}^2} = \sqrt{\sum_m P_m \langle \phi_m | \hat{X}_\eta^2 | \phi_m \rangle}, \tag{28}$$

where ϕ_n is the n^{th} Harmonic oscillator stationary state, and P_n is the corresponding Boltzmann-weighted probability at T = 298 K. (3) We estimate the change in diabatic coupling with respect to this degree of freedom ($\Delta H_{AB,\eta}$) as the product of the component of the gradient along this degree of freedom with the magnitude of the fluctuation along this degree of freedom, $\Delta H_{AB,\eta} = \Delta L_\eta H_{AB}^{[\eta]}$.

Using this procedure, we can calculate $\Delta H_{AB,\eta}$ across all degrees of freedom by examining the projection of the gradient vectors onto each normal mode of the ground state. For the $\zeta = 0$ configuration, we find that there are 5 modes along which the diabatic coupling could change by more than 20% of its reference value. The most significant of these is mode 59; our analysis suggests that the diabatic coupling could change by 33% if the molecule were to move along this degree of freedom at room temperature. For the $\zeta = 1$ configuration, there are only 3 modes which the diabatic coupling could change by more than 20%; mode 59 is also the most significant in this case, along which the diabatic coupling can change by 31%.

TABLE II: Analysis of change in diabatic coupling of C-1,4ee due to thermally-induced conformational fluctuations at T = 298 K along the normal modes which contribute most significantly to ΔH_{AB}. The curvature around each potential energy well on the T_1 surface is taken to be the same as that of the S_0 minimum, and is obtained from a ground-state Hessian calculation. Using this information, we are able to estimate how much this molecule can be expected to deviate (ΔL) from its stable configurations ($\zeta = 0$ and $\zeta = 1$) at room temperature. Multiplying this value by the projection of the diabatic coupling gradient ($|H_{AB}^{[\eta]}|$) tells us how much we can then expect the diabatic coupling to change ($\Delta H_{AB,\eta}$) both in absolute terms and as a fraction of its value at the respective reference configuration (H_{AB}).

Configuration	H_{AB} (μE_h)	mode (η)	$\lvert H_{AB}^{[\eta]}\rvert$ ($\mu E_h/a_0$)	ΔL_η (a_0)	$\Delta H_{AB,\eta}$ (μE_h)	$\Delta H_{AB,\eta}$ (%)
$\zeta = 0$	22.4	59	45.7	0.162	7.39	33.1
		57	34.8	0.157	5.48	24.5
		77	34.4	0.145	4.99	22.3
		106	67.8	0.072	4.91	22.0
		65	30.5	0.149	4.55	20.4
$\zeta = 1$	22.1	59	42.6	0.162	6.89	31.1
		57	42.4	0.157	6.67	30.2
		109	72.3	0.074	5.35	24.2
		73	22.1	0.177	3.91	17.7
		82	21.5	0.181	3.88	17.5

For a visual representation of the normal modes which correspond to the greatest change in the diabatic coupling, see Fig. 5.

Under the approximation described in this section, one can calculate the total change in diabatic coupling ($\Delta H_{AB}^{\text{total}}$) as the 2-norm of its component parts,

$$\Delta H_{AB}^{\text{total}} = \sqrt{\sum_{\eta} (\Delta H_{AB,\eta})^2}. \tag{29}$$

For the $\zeta = 0$ configuration, $\Delta H_{AB}^{\text{total}} = 19$ μE_h, or a 87% change from the reference value.

For the $\zeta = 1$ configuration, $\Delta H_{AB}^{\text{total}} = 17\ \mu\text{E}_\text{h}$, a 78% change. Because of these fluctuations in the electronic coupling alone, we can expect our calculated Marcus rates to be off by up to a factor of 3 or 4 from the experimental rates. In our view, however, such small effects do not represent a significant breakdown of the Condon approximation; indeed, as a practical matter, the original calculations in Ref. 28 were also off by a factor of 2 to 3 from the experimental results. In the end, while there may be some fluctuations of the diabatic coupling, the molecule is rigid enough at room temperature that non-Condon effects will be relatively small.

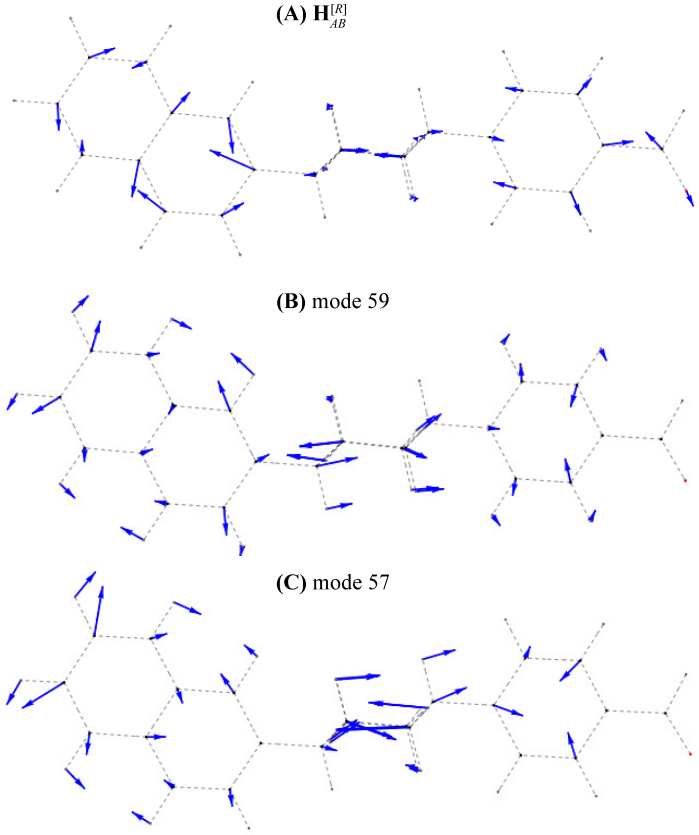

FIG. 5: Quiver plot of C-1,4ee depicting the **(A)** diabatic coupling gradient ($\mathbf{H}_{AB}^{[R]}$) at $\zeta = 0$, **(B)** normal mode 59 from the S_0 minimum-energy configuration, and **(C)** normal mode 57 from the S_0 minimum-energy configuration. Those modes are each moderately rigid, with characteristic lengths $\Delta L_{59} = 0.162\ \text{a}_0$ and $\Delta L_{57} = 0.157\ \text{a}_0$. At the $\zeta = 0$ geometry, the projection of the diabatic coupling gradient ($H_{AB}^{[\eta]}$) onto mode 59 is $H_{AB}^{[59]} = 45.7\ \mu\text{E}_\text{h}/\text{a}_0$, and $H_{AB}^{[57]} = 34.8\ \mu\text{E}_\text{h}/\text{a}_0$ for mode 57. At the $\zeta = 1$ geometry, $H_{AB}^{[59]} = 42.6\ \mu\text{E}_\text{h}/\text{a}_0$, and $H_{AB}^{[57]} = 42.4\ \mu\text{E}_\text{h}/\text{a}_0$. See Table II for a thorough description of how these quantities are determined.

V. DISCUSSION: THE STRICTLY DIABATIC APPROXIMATION

To test the viability of the strictly diabatic approximation described in section III C, we have used it to to calculate the Hamiltonian gradient in the BoysOV basis ($\mathbf{H}^{[R]}$) for C-1,4ee. To more clearly assess this approximation of a vector quantity, error analysis has been split into two components: magnitude and direction. Magnitudinal error is calculated as the conventional error for scalar quantities,

$$\varepsilon_{\text{mag}} = \frac{|\mathbf{H}^{[R]}_{AB,\text{approx.}}| - |\mathbf{H}^{[R]}_{AB,\text{analytic}}|}{|\mathbf{H}^{[R]}_{AB,\text{analytic}}|}. \tag{30}$$

Directional error is obtained by normalizing both the approximate and analytic vector quantities, then subtracting their inner product from unity,

$$\varepsilon_{\text{dir}} = 1 - \left(\frac{\mathbf{H}^{[R]}_{AB,\text{approx.}}}{|\mathbf{H}^{[R]}_{AB,\text{approx.}}|}\right) \cdot \left(\frac{\mathbf{H}^{[R]}_{AB,\text{analytic}}}{|\mathbf{H}^{[R]}_{AB,\text{analytic}}|}\right). \tag{31}$$

First, we discuss diabatic coupling gradients ($\mathbf{H}^{[R]}_{AB}$, $A \neq B$). A comparison between these results and those found for direct analytic evaluation of the diabatic coupling gradient can be found in Fig. 6.

Under the strictly diabatic approximation, the diabatic coupling gradient is accurately approximated near the avoided crossing at $\zeta = 0.89$. For the region $0.8 < \zeta < 1.0$, the magnitudinal error in the diabatic coupling vector diverges linearly away from the avoided crossing, ultimately rising to 4%. In this same region, the directional error is generally much smaller; with the exception of a spike to 2% at the geometry nearest to the avoided crossing, the directional error does not rise past 0.2%. Further away from the avoided crossing, the approximation fares much worse: for $\zeta < 0.5$, the magnitudinal error is greater than 10%, and the directional error rises to nearly 50% for $\zeta = 0$. Of course, the relatively large error at the $\zeta = 0$ configuration compared to the $\zeta = 1$ configuration reflects only

the relative distance from the avoided crossing. These data strongly suggest, as one might expect, that the strictly diabatic approximation should be used only at configurations where the derivative coupling in the localized diabatic basis is significantly smaller than in the adiabatic basis, i.e., near avoided crossings (see Fig. 2).

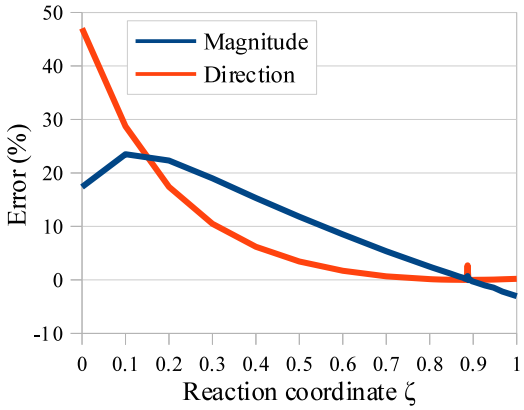

FIG. 6: Error in the magnitude and direction of the diabatic coupling gradient ($\mathbf{H}^{[R]}_{AB}$) under the strictly diabatic approximation along the linearly-interpolated reaction pathway between A*D ($\zeta = 0$) and AD* ($\zeta = 1$) T_1 states of the C-1,4ee molecule. Magnitudinal error is calculated as the conventional relative change for scalar quantities (Eq. 30). Directional error is obtained by normalizing both the approximate and true vector quantities, then subtracting their inner product from unity (Eq. 31). While both magnitudinal and directional errors are very low near the avoided crossing (at $\zeta = 0.89$), they begin to diverge significantly for $\zeta < 0.6$. While the error in the magnitude has a maximum of around 25%, the directional error is nearly 50% and rising as $\zeta \to 0$. This strongly suggests that for diabatic couplings, this approximation is only reliable where diabatization can achieve significant reductions in DC magnitudes, i.e. near avoided crossings.

Second, we study diabatic energy gradients ($\mathbf{H}^{[R]}_{AA}$). In contrast to the results for the diabatic coupling gradients, the approximate diabatic state energy gradients are essentially identical to the analytic result for every point sampled. For much of configuration space, this be attributed to the fact that the dominant contribution to the diabatic energy gradient comes from the first term on the right hand side of Eq. 26, which does not depend on $\mathbf{U}^{[R]}$, and is therefore unchanged by the approximation. Near the avoided crossing, however, $\mathbf{U}$ changes rapidly, and the remaining terms in this expression can no longer be neglected. In this region, however, the derivative couplings in the diabatic representation are smallest, so

the strictly diabatic approximation is the most well-founded. Thus, in two complementary limits, it seems that the strictly diabatic approximation for energy gradients can be expected to be accurate. As it turns out, the error in the approximate magnitude of the gradient is never much greater than $10^{-4}\%$, and directional error never rises above $10^{-9}\%$. For energy gradients, at least, the strictly diabatic approximation appears to be extremely robust.

VI. CONCLUSIONS AND FUTURE WORK

The recent advent and implementation of analytic gradient methods for localized diabatic states has been tremendously helpful in both evaluating the reliability of these quasi-diabatic representations, and increasing the functionality of these transformations. In this work, we used methods introduced in Ref. 30 to evaluate the properties of diabatic states of triplet-triplet energy transfer systems, finding that the derivative couplings were negligible and that diabatic couplings were largely stable. Furthermore, we extended these methods to encompass BoysOV and GMH states. Finally, we used the knowledge that derivative couplings in the diabatic basis are reliably small to propose an approximation that allows diabatic gradient quantities to be calculated at greatly reduced cost. We were able to show that this 'strictly diabatic' approximation was successful at accurately calculating diabatic coupling gradients near avoided crossings, and diabatic energy gradients everywhere. We fully expect that these results are transferable to the gradients of other observables.

Looking forward, we anticipate that the strictly diabatic approximation may make several new applications of these diabatic gradient methods more attractive. One such application is diabatic state energy minimization: because local minima on an adiabatic potential energy surface may correspond to global minima on a diabatic potential energy surface, performing a geometry optimization on diabatic surfaces may offer a more reliable way to find such

configurations. We plan to implement and make available this technique in the coming months.

VII. ACKNOWLEDGMENTS

This work was supported by NSF CAREER Grant CHE-1150851. J.E.S. acknowledges an Alfred P. Sloan Research Fellowship and a David & Lucile Packard Fellowship.

Appendix A: Generalization of BoysOV

While the Boys representation is defined in terms of the excitation dipole matrix, X_{AB}, the BoysOV representation is defined in terms of partitions of the this matrix, including the occupied component X_{AB}^{occ}, and the virtual component X_{AB}^{virt}, such that their sum equals the full excitation dipole matrix, $X_{AB} = X_{AB}^{\text{occ}} + X_{AB}^{\text{virt}}$. This partitioning is trivially defined for CIS and TD-DFT/TDA because both of these methods involve only single excitations from a reference ground state (see Eqs. 7 and 8). For any more sophisticated wavefunction ansatz, however, the partitioning process is not as clear.

Although it may not always be physical, a reasonable partitioning of the dipole matrix can be defined, provided there is a single determinant reference ground state. For example, one can write state dipole matrix elements in the molecular orbital basis,

$$X_{AB} = \sum_{r,s} X^{rs} D_{AB}^{rs} \tag{A1}$$

for some excitation density matrix $\mathbf{D}$. The density matrix can be split into occupied and

virtual components, $D^{rs}_{AB} = D^{rs,\mathrm{occ}}_{AB} + D^{rs,\mathrm{virt}}_{AB}$ as follows:

$$D^{rs,\mathrm{occ}}_{AB} = \begin{cases} D^{rs}_{AB} & \text{if } r,s \in \text{ occ}, \\ \frac{1}{2} D^{rs}_{AB} & \text{if } r \in \text{ occ and } s \in \text{ virt, or } s \in \text{ occ and } r \in \text{ virt, and} \\ 0 & \text{if } r,s \in \text{ virt}, \end{cases} \tag{A2}$$

with $D^{rs,\mathrm{virt}}_{AB}$ defined in an analogous manner. The occupied and virtual components of the dipole matrix can then be written as

$$X^{\mathrm{occ}}_{AB} = \sum_{r,s} X^{rs} D^{rs,\mathrm{occ}}_{AB} \tag{A3}$$

and

$$X^{\mathrm{virt}}_{AB} = \sum_{r,s} X^{rs} D^{rs,\mathrm{virt}}_{AB}. \tag{A4}$$

---

[1] Matsika, S.; Krause, P. *Annual Review of Physical Chemistry* **2011**, *62*, 621–643.

[2] Mead, C. A.; Truhlar, D. G. *The Journal of Chemical Physics* **1982**, *77*, 6090–6098.

[3] Van Voorhis, T.; Kowalczyk, T.; Kaduk, B.; Wang, L.-P.; Cheng, C.-L.; Wu, Q. *Annual Review of Physical Chemistry* **2010**, *61*, 149–170.

[4] Baer, M. *Chemical Physics Letters* **1975**, *35*, 112 – 118.

[5] Sadygov, R. G.; Yarkony, D. R. *The Journal of Chemical Physics* **1998**, *109*, 20–25.

[6] Zhu, X.; Yarkony, D. R. *The Journal of Chemical Physics* **2010**, *132*, 104101.

[7] Pacher, T.; Cederbaum, L. S.; Köppel, H. In *Adiabatic and Quasiadiabatic States in a Gauge Theoretical Framework*; Prigogine, I., Rice, S. A., Eds.; Advances in Chemical Physics; Wiley, 1993; Vol. 84; pp 293–391.

[8] Ruedenberg, K.; Atchity, G. J. *The Journal of Chemical Physics* **1993**, *99*, 3799–3803.

[9] Atchity, G. J.; Ruedenberg, K. *Theoretical Chemistry Accounts: Theory, Computation, and Modeling (Theoretica Chimica Acta)* **1997**, *97*, 47–58.

[10] Nakamura, H.; Truhlar, D. G. *The Journal of Chemical Physics* **2001**, *115*, 10353–10372.

[11] Nakamura, H.; Truhlar, D. G. *The Journal of Chemical Physics* **2002**, *117*, 5576–5593.

[12] Nakamura, H.; Truhlar, D. G. *The Journal of Chemical Physics* **2003**, *118*, 6816–6829.

[13] Cave, R. J.; Newton, M. D. *Chemical Physics Letters* **1996**, *249*, 15 – 19.

[14] Cave, R. J.; Newton, M. D. *The Journal of Chemical Physics* **1997**, *106*, 9213–9226.

[15] Yarkony, D. *Journal of Physical Chemistry A* **1998**, *102*, 8073–8077.

[16] Yarkony, D. *Journal of Chemical Physics* **1999**, *110*, 701–705.

[17] Kryachko, E. S.; Yarkony, D. R. *International Journal of Quantum Chemistry* **2000**, *76*, 235–243.

[18] Voityuk, A. A.; Rösch, N. *The Journal of Chemical Physics* **2002**, *117*, 5607–5616.

[19] Hsu, C.-P.; You, Z.-Q.; Chen, H.-C. *The Journal of Physical Chemistry C* **2008**, *112*, 1204–1212.

[20] Chen, H.-C.; You, Z.-Q.; Hsu, C.-P. *The Journal of Chemical Physics* **2008**, *129*, 084708.

[21] Hsu, C.-P. *Accounts of Chemical Research* **2009**, *42*, 509–518.

[22] Wu, Q.; Van Voorhis, T. *The Journal of Physical Chemistry A* **2006**, *110*, 9212–9218.

[23] Wu, Q.; Voorhis, T. V. *The Journal of Chemical Physics* **2006**, *125*, 164105.

[24] Wu, Q.; Van Voorhis, T. *Journal of Chemical Theory and Computation* **2006**, *2*, 765–774.

[25] Newton, M. D. *Chemical Reviews* **1991**, *91*, 767–792.

[26] Subotnik, J. E.; Yeganeh, S.; Cave, R. J.; Ratner, M. A. *The Journal of Chemical Physics* **2008**, *129*, 244101.

[27] Subotnik, J. E.; Cave, R. J.; Steele, R. P.; Shenvi, N. *The Journal of Chemical Physics* **2009**,

130, 234102.

[28] Subotnik, J. E.; Vura-Weis, J.; Sodt, A. J.; Ratner, M. A. *The Journal of Physical Chemistry A* **2010**, *114*, 8665–8675.

[29] Alguire, E.; Subotnik, J. E. *The Journal of Chemical Physics* **2012**, *137*, 194108.

[30] Fatehi, S.; Alguire, E.; Subotnik, J. E. *The Journal of Chemical Physics* **2013**, *139*, 124112.

[31] Granucci, G.; Persico, M.; Toniolo, A. *The Journal of Chemical Physics* **2001**, *114*, 10608–10615.

[32] Plasser, F.; Granucci, G.; Pittner, J.; Barbatti, M.; Persico, M.; Lischka, H. *The Journal of Chemical Physics* **2012**, *137*, 22A514.

[33] Tully, J. C. *The Journal of Chemical Physics* **1990**, *93*, 1061–1071.

[34] Kapral, R.; Ciccotti, G. *The Journal of Chemical Physics* **1999**, *110*, 8919–8929.

[35] Ben-Nun, M.; Martínez, T. J. *The Journal of Chemical Physics* **2000**, *112*, 6113–6121.

[36] Ananth, N.; Venkataraman, C.; Miller, W. H. *The Journal of Chemical Physics* **2007**, *127*, 084114.

[37] Closs, G. L.; Piotrowiak, P.; MacInnis, J. M.; Fleming, G. R. *Journal of the American Chemical Society* **1988**, *110*, 2652–2653.

[38] Closs, G. L.; Johnson, M. D.; Miller, J. R.; Piotrowiak, P. *Journal of the American Chemical Society* **1989**, *111*, 3751–3753.

[39] Fatehi, S.; Alguire, E.; Shao, Y.; Subotnik, J. E. *The Journal of Chemical Physics* **2011**, *135*, 234105.

[40] Lengsfield, B. H.; Yarkony, D. R. *Advances in Chemical Physics* **1992**, *82*, 1–71.

[41] Yarkony, D. R. *Conical Intersections in Electron Photodetachment Spectroscopy: Theory and Applications*; Advanced Series in Physical Chemistry; World Scientific, 2004; Vol. 15; pp

129–174.

[42] Lengsfield, B. H.; Saxe, P.; Yarkony, D. R. *The Journal of Chemical Physics* **1984**, *81*, 4549–4553.

[43] Saxe, P.; III, B. H. L.; Yarkony, D. R. *Chemical Physics Letters* **1985**, *113*, 159 – 164.

[44] Lischka, H.; Dallos, M.; Shepard, R. *Molecular Physics* **2002**, *100*, 1647–1658.

[45] Lischka, H.; Dallos, M.; Szalay, P. G.; Yarkony, D. R.; Shepard, R. *The Journal of Chemical Physics* **2004**, *120*, 7322–7329.

[46] Dallos, M.; Lischka, H.; Shepard, R.; Yarkony, D. R.; Szalay, P. G. *The Journal of Chemical Physics* **2004**, *120*, 7330–7339.

[47] Jørgensen, P.; Simons, J. *The Journal of Chemical Physics* **1983**, *79*, 334–357.

[48] Helgaker, T. U.; Almlöf, J. *International Journal of Quantum Chemistry* **1984**, *26*, 275–291.

[49] Page, M.; Saxe, P.; Adams, G. F.; Lengsfield, B. H. *The Journal of Chemical Physics* **1984**, *81*, 434–439.

[50] Shepard, R. *International Journal of Quantum Chemistry* **1987**, *31*, 33–44.

[51] Shepard, R.; Lischka, H.; Szalay, P. G.; Kovar, T.; Ernzerhof, M. *The Journal of Chemical Physics* **1992**, *96*, 2085–2098.

[52] Shao, Y. et al. *Phys. Chem. Chem. Phys.* **2006**, *8*, 3172–3191.

[53] Krylov, A. I.; Gill, P. M. W. *WIREs Comput. Mol. Sci.* **2013**, *3*, 317–326.

[54] Nitzan, A. *Chemical Dynamics in Condensed Phases*; Oxford University Press: New York, 2006.

[55] Ratner, M.; Schatz, G. *Quantum Mechanics in Chemistry*; Dover Publications: Mineola, NY, 2002.